Chemico-Biological Interactions 241 (2015) 76–86

Contents lists available at ScienceDirect

Chemico-Biological Interactions

journal homepage: www.elsevier.com/locate/chembioint

Novel and existing data for a future physiological toxicokinetic model of ethylene and its metabolite ethylene oxide in mouse, rat, and human

Johannes Georg Filser [a,b,*], Anna Artati [a], Qiang Li [a], Christian Pütz [a], Brigitte Semder [a], Dominik Klein [a,b], Winfried Kessler [a]

[a] Institute of Molecular Toxicology and Pharmacology, Helmholtz Zentrum München, Neuherberg, Germany
[b] Institut für Toxikologie und Umwelthygiene, Technische Universität München, München, Germany

ARTICLE INFO

Article history:
Available online 10 April 2015

Keywords:
Ethylene
Ethylene oxide
Mouse
Rat
Human

ABSTRACT

The olefin ethylene is a ubiquitously found gas. It originates predominantly from plants, combustion processes and industrial sources. In mammals, inhaled ethylene is metabolized by cytochrome P450-dependent monooxygenases, particularly by cytochrome P450 2E1, to ethylene oxide, an epoxide that directly alkylates proteins and DNA. Ethylene oxide was mutagenic in vitro and in vivo in insects and mammals and carcinogenic in rats and mice. A physiological toxicokinetic model is a most useful tool for estimating the ethylene oxide burden in ethylene-exposed rodents and humans. The only published physiological toxicokinetic model for ethylene and metabolically produced ethylene oxide is discussed. Additionally, existing data required for the development of a future model and for testing its predictive accuracy are reviewed and extended by new gas uptake studies with ethylene and ethylene oxide in B6C3F1 mice and with ethylene in F344 rats.

1. Introduction

1.1. Sources of ethylene

The olefin ethylene (ET; CAS No.: 74-85-1) is a gas found ubiquitously in the environment. It is produced by microorganisms, fungi, and plants (see, e.g., [74,40,89]. Mammals exhale endogenously formed ET (mice, [56]; rats, [82]; humans, [75,15,82,34]. ET is the largest volume chemical produced globally [1]. It is primarily used in the production of polymers and industrial chemicals. About 74% of environmental atmospheric ET was related to natural and 26% to anthropogenic sources. Important environmental sources of ET are natural fires and man-made combustion of organic material as well as releases during its production and use (reviewed, e.g., in [45,2]. Concentrations of ET in ambient air are generally below 15 μg/m^3 (about 13 ppb) in rural areas and can amount to up to 805 μg/m^3 in cities [2]. In the air of a fruit store ET concentrations were in the range of 0.02–3.35 ppm [88]. A concentration of 46 ppm of ET was measured during firefighting [51]. ET concentrations of up to 47 mg/m^3 (about 40 ppm) were reported in a Swedish plastic producing company [41]. In a Canadian ET production facility, general workplace exposures to ET were below 15 ppm [67]. Field measurements performed at 14 petrochemical facilities in North America revealed a mean 8-h time weighted average atmospheric ET concentration of 2.6 ppm (range <0.05–2100 ppm). In two of the 146 samples collected during 4-h periods, average 4-h concentrations of atmospheric ET were 3200 and 4200 ppm [61].

1.2. Biological fate of ET

ET is only slightly soluble in water (Ostwald coefficient of 0.1198 at 101.325 kPa and 25 °C; [81]). Its blood/air partition coefficient,

Abbreviations: CYP, cytochrome P450-dependent monooxygenase(s); CYP2E1, cytochrome P-450 2E1; dithiocarbamate, sodium diethyldithiocarbamate trihydrate; EH, epoxide hydrolase; ET, ethylene; EO, ethylene oxide; GC/FID, gas chromatograph equipped with flame ionization detector; GSH, glutathione; GST, glutathione S-transferase; GSTT1, GST class Theta 1; K_{eq}, partition coefficient whole organism/air; k_{GSH}, pseudo first-order rate constant of the spontaneous conjugation of EO with GSH; k_{hydrol}, first-order rate constant of the non-enzymatic hydrolysis of EO; k_{inhib}, first-order rate constant of the ET-mediated suicide inhibition of CYP2E1; K_m, apparent Michaelis constant; K_{mCYP}, apparent Michaelis constant of CYP2E1-catalyzed EO formation; K_{mEH}, apparent Michaelis constant of epoxide hydrolase-catalyzed EO hydrolysis; K_{mGST}, apparent Michaelis constant of GST-catalyzed conjugation of EO with GSH; PT model, physiological toxicokinetic model; V_{max}, maximum rate of metabolism; V_{maxCYP}, maximum rate of CYP2E1-catalyzed EO formation from ET; V_{maxEH}, maximum rate of epoxide hydrolase-catalyzed EO hydrolysis; V_{maxGST}, maximum rate of GST-catalyzed conjugation of EO with GSH; V_1, volume of the air space in a closed exposure chamber; V_2, volume of the sum of the animals exposed in a closed chamber.

* Corresponding author at: Institute of Molecular Toxicology and Pharmacology, Helmholtz Zentrum München, Ingolstädter Landstrasse 1, 85764 Neuherberg, Germany. Tel.: +49 89 3187 2977; fax: +49 89 3187 3449.

E-mail address: johannes.filser@helmholtz-muenchen.de (J.G. Filser).

http://dx.doi.org/10.1016/j.cbi.2015.04.002
0009-2797/

determined at 37 °C, was low: 0.48 in rodents and 0.22 in humans [20]. As a consequence, the major part of ET inhaled by rats and humans was exhaled unchanged, only a minor part was metabolized. The pulmonary retention or the 1.5 times larger alveolar retention of ET at steady state (criteria for the metabolism of inhaled gases; see, e.g., [36]) were below 10% in humans and in rats [35,33]. In mammals, ET is biotransformed to ethylene oxide (EO, CAS No.: 75-21-8). The epoxide was detected in ET-exposed mice, rats, and humans [31,32,60,30,35]. The formation of EO from ET is catalyzed by cytochrome P450-dependent monooxygenase(s) (CYP) as was shown in liver microsomes of the same species [83,58]. Hydroxyethyl-adducts to hemoglobin and DNA, which are characteristic for EO, were quantified in ET-exposed rodents and hydroxyethyl-adducts to hemoglobin in ET-exposed humans (summarized in, e.g., [35]). Metabolic elimination of EO proceeds in subcellular liver fractions of mice and rats predominantly via conjugation with glutathione (GSH) mediated by hepatic cytosolic glutathione S-transferase (GST) as was shown by [11] and [58]. In human liver subcellular fractions, microsomal epoxide hydrolase (EH) plays a pivotal role for the metabolic elimination of EO, too [58].

1.3. Mutagenicity and carcinogenicity of EO

EO, a colorless gas at room temperature (boiling point: 10.8 °C at 101.3 kPa), is a high production volume chemical used primarily as an intermediate in the synthesis of various chemicals, especially ethylene glycol. A very minor part is used as fumigant and insecticide and as sterilizing agent, e.g., for food and medical devices (see, e.g., [46,47,48]). EO is a directly protein- and DNA-alkylating agent (reviewed in, e.g., [97]). It was mutagenic in vitro in bacteria and cells of animals and humans and in vivo in mice, rats, monkeys (reviewed, e.g., in [47]), and Drosophila [66]. Increased frequencies of micronucleated cells were found in EO-exposed mice, rats, and humans. In mice and rats, EO was carcinogenic (summarized in, e.g., [47,48]). IARC [48] evaluated EO as carcinogenic to humans (Group 1) by taking into account the "sufficient evidence for the carcinogenicity of ethylene oxide in experimental animals" and relying "heavily on the compelling data in support of the genotoxic mechanism" of EO.

1.4. Mutagenicity and carcinogenicity of ET

Despite its metabolism to EO, ET was neither mutagenic in Salmonella Typhimurium [91] nor mutagenic/genotoxic in rodents [90,94] nor carcinogenic in F344 rats that were long-term exposed to ET concentrations of up to 3000 ppm [43]. The negative results of the latter study agree with the suggestion that the tissue burdens of metabolically formed EO were too low to produce significant effects in a standard carcinogenicity study with ET [8,71,94].

1.5. Rationale for developing a physiological toxicokinetic model for ET and its metabolite EO in rodents and humans

A physiological toxicokinetic (PT) model for ET and its metabolite EO in mice, rats, and humans should reproduce quantitative differences in the tissue burdens by ET and EO between the three species. It should assess internal exposures to EO in relation to external EO concentrations for which dose–responses of carcinogenic effects were reported in both rodent species. In addition, it should "reflect interindividual differences in activation and clearance of the reactive epoxides" as has been asked by Melnick [63] when he was dealing with cancer risks from several olefins including ET. This statement is most relevant with respect to the kinetics of EO which is metabolically eliminated by GST class Theta 1 (GSTT1). The enzyme shows genetic polymorphism in humans, which may result in sub-population-specific kinetics of EO [87]. However, such a PT model has to be validated on experimental in vivo data in order to be considered as accurate and reliable: over a range of doses the predicted fate of the chemical (ET) and its toxicologically relevant metabolite (EO) in the body (blood, plasma, or other tissues) should agree with experimental data in laboratory animals and humans [17].

1.6. Aim of the present work

It was the aim of the present work to review the only published PT model for ET and its metabolite EO and to discuss newer data that will be most useful for the development of a revised PT model and for testing its predictive accuracy in the EO burden of ET-exposed B6C3F1 mice, F344 rats, and GSTT1 positive and negative humans. In addition, some novel gas uptake studies with ET and EO in B6C3F1 mice and with ET in F344 rats are to be presented. They will serve to validate model-predicted elimination kinetics of ET in both strains and of EO in B6C3F1 mice. A gas uptake study with EO in F344 rats was not carried out because such a study has already been published [55]. F344 rats were used in the carcinogenicity study with inhaled ET [43], B6C3F1 mice and F344 rats in carcinogenicity studies with inhaled EO (F344 rats: [37,38,59,84]; B6C3F1 mice: [68]).

2. Materials and methods

2.1. Chemicals

Synthetic air 5.5, helium 5.0, hydrogen 5.0, oxygen 4.5, nitrogen 5.0, ET 3.5, and EO 3.0 were obtained from Linde, Unterschleissheim, Germany. Soda lime "Drägersorb 800Plus" was from Drägerwerk, Lübeck, Germany, and sodium diethyldithiocarbamate trihydrate (dithiocarbamate) from Sigma–Aldrich, Taufkirchen, Germany.

2.2. Animals

Male F344 rats (in vivo studies, body weights: 280–320 g; control experiments with carcasses, body weights: 232 and 258 g) and male B6C3F1 mice (body weights: 25–30 g) were from Charles River Wiga Deutschland, Sulzfeld, Germany. Animal husbandry and experimental procedures were performed in conformity with the "Guide for the Care and Use of Laboratory Animals" [65]. In order to acclimate the animals, groups of 2 rats or 5 mice, respectively, were housed for at least 5 days before use in a Makrolon type III cage which was placed in an IVC top flow system (Tecniplast, Buguggiate, Italy). This system provided the animals with HEPA-filtered air of 22–25 °C and 50–60% humidity. A constant 12-h light/dark cycle was maintained in the chamber room. Animals had free access to standard chow (Nr. 1324 from Altromin, Lage, Germany) and tap water.

2.3. Inhalation studies in mice and rats

Before carrying out gas-uptake studies with ET or EO in closed all-glass exposure chambers, it was tested whether the presence of soda lime—required for adsorbing exhaled CO_2—leads to a loss of the concentration of ET or EO in chamber air. Closed chambers (about 2.8 L for ET and about 6.4 L for EO) contained 25 g of soda lime per chamber. The soda lime had been humidified with urine and exhaled water by exposing 5 mice per chamber to pure air for 5 h. After removing the animals from the chambers, initial concentrations of ET and EO were adjusted to 1090 ppm and 94 ppm, respectively, and concentration–time courses were monitored for about 7 h (both gases). In order to check whether skin and body of the animals influence the gas concentration of ET or EO in the

chamber air, 5 carcasses of B6C3F1 mice were exposed to ET (initial atmospheric concentration 30.4 ppm) or to EO (initial concentration 26.5 ppm) in closed soda lime (25 g) containing chambers of about 2.8 L (ET exposure) or 6.4 L (EO exposure), and the concentration–time courses of ET or EO were monitored up to 7 h. Also, 2 carcasses of F344 rats (average body weight: 245 g) were exposed for 6 h to ET (initial concentration 30 ppm) in a closed soda lime (30 g) containing chamber (6.4 L).

For studying the gas uptake of ET or EO, naïve animals were exposed in closed chambers that contained soda lime for adsorbing exhaled CO_2. The resulting loss of CO_2 from the chamber air was continuously compensated by oxygen. The exposure system and the automatic oxygen supply are described in detail in [33]. Five male B6C3F1 mice per group (average body weight: 27.5 g) were exposed for about 7 h to either ET or EO. The ET experiments were started by injecting defined amounts of the gas into the atmosphere of the exposure chambers (volume: 2.8 L; amount of soda lime: 25 g) that resulted at initial concentrations of 1.1, 3.0, 11, 33, 83, 330, 1050, 3110, or 11,200 ppm. Male F344 rats (average body weight: 300 g) were exposed to ET for 6 h in groups of 2 animals. The exposure chambers of 6.4 L contained 30 g of soda lime. Initial atmospheric ET concentrations of 34, 105, 295, 1090, 3110, or 10,500 ppm were established by injecting the required amount of ET into the chamber atmosphere. For the gas uptake studies with EO-exposed mice (groups of 5 animals per exposure experiment; average body weight: 27.5 g), chambers of 6.4 L were used which contained 25 g of soda lime. Gaseous EO was injected at initial concentrations of 8.8, 27, 106, 360, 980, or 2700 ppm into the chamber air.

In order to determine the thermodynamic equilibrium between the animal body and the atmospheric ET concentration (the maximum enrichment of inhaled ET in the organism), 5 animals of each of both species were pretreated with dithiocarbamate, an inhibitor of CYP2E1 (e.g., [42,85]). Of a solution containing 50 mg dithiocarbamate per ml of physiological saline, doses of dithiocarbamate of 400 and of 200 mg per kg of body weight were administered intraperitoneally to mice and rats, respectively, 30 min before starting the exposures to ET. The pretreated 5 mice (average body weight: 27.5 g) were exposed together for 2 h in a soda lime (25 g) containing closed chamber of 0.8 L starting with an initial ET concentration of about 10 ppm. The group of 5 rats (average body weight: 300 g) was exposed for 2.75 h in a soda lime (30 g) containing chamber of 6.4 L. The initial ET concentration in the chamber air was 430 ppm. The relatively small chamber sizes compared to the animal volumes established a high sensitivity concerning the loss of the ET concentration in air.

2.4. Gas chromatography

Atmospheric concentrations of ET or EO were determined using gas chromatographs equipped with flame ionization detectors (GC/FID), gas sample loops, and stainless steel columns (3.5 m × 2 mm ID) packed with Tenax TA (60–80 mesh). Chromatographic separations were done isothermally. The GC/FID-procedures are described in detail in [35] ("GC/FID method A" for ET and "GC/FID method B" for EO). Unfortunately, in the cited publication the column temperature and the carrier gas pressure used for the determination of ET were given incorrectly. The correct values were 60 °C and 2.5 kg/cm^2.

3. Results and discussion

3.1. Existing PT model for ET

The only PT model for ET was developed by Csanády et al. [20]. It was used to predict concentration–time courses of ET or EO in ET- or EO-exposed rodents or humans and of exhaled EO in ET-exposed rats. The model described also the formation and elimination of 2-hydroxyethyl adducts to hemoglobin and DNA in ET- or EO-exposed rodents and humans and, in addition, the endogenous production of ET in rats and humans. Modeled compartments represented arterial, venous, and pulmonary blood, muscle, fat, richly perfused tissues, and the liver as the only metabolizing organ. Physiological parameters were taken from the literature (most of them from [5]). Partition coefficients of ET and EO were determined experimentally. The maximum rate of ET metabolism and the corresponding apparent Michaelis constant were obtained for rats by fitting the model to gas uptake data in ET-exposed male Sprague–Dawley rats [6]. For mice, the maximum rate of ET metabolism was allometrically extrapolated from the rat value using a surface scaling factor of (body weight)$^{2/3}$; the value of the apparent Michaelis constant was the same as in rats, assuming the enzymatic properties to be the same in both species. For humans, a clearance value was gained by model fits to data measured in ET-exposed volunteers [23,34]. Metabolic elimination of EO was expressed by a clearance the numerical value of which was derived by model fits to concentration–time courses of EO in the blood of EO-exposed F344 rats [11]. For mice and humans, clearance values of EO elimination were obtained from the rat value by allometric scaling using a surface factor of (body weight)$^{2/3}$. Production rates of endogenous ET were obtained in rats and humans by model fits to data reported by Denk [23] and Filser et al. [34]. Rate constants of adduct formation and elimination, required to predict 2-hydroxyethyl adducts of hemoglobin and DNA, were taken from the literature [79,80,25,92].

In order to validate the PT model, predicted concentration–time courses of ET or EO were compared to measured ones. These were concentration–time courses of ET in exhaled air of Sprague–Dawley rats after intraperitoneal administration of ET [6], of exhaled EO in Sprague–Dawley rats exposed to high ET concentrations (>1000 ppm; [32]), of EO in gas uptake studies in EO-exposed F344 rats [55] or Sprague–Dawley rats [32], of EO in blood of EO-exposed B6C3F1 mice [12], and of EO in the atmosphere of an exposure chamber during and after EO exposure of (C3H/R1xB110/R1)F_1 hybrid mice [78]. For humans, predicted EO concentrations in blood and in exhaled air of EO-exposed workers were compared to data measured by Brugnone et al. [13,14]. Additionally, predicted levels of 2-hydroxyethyl adducts of hemoglobin and DNA were compared with data that had been measured in mice, rats, and humans exposed to ET (mouse: [96]; rat: [26,96]; human: [88,53,34]) or EO (mouse: [79,92,93,95]; rat: [72,73,92,93,95]; human: [24,57,4,10]).

Model simulations of concentrations of ET or EO in blood, in exhaled air, or in the air in gas uptake studies agreed with data measured in ET- or EO-exposed rodents and humans. Also, predicted DNA adduct levels in rodents agreed with reported ones. However, hemoglobin adduct levels were underpredicted in rodents by a factor of 2–3. Also, concentration–time courses of exhaled EO that was formed metabolically in rats from inhaled ET at high exposure concentrations (>1000 ppm) was not predicted correctly because the initial EO peak could not be described by the model (Fig. 1). The model could not be improved for metabolically produced EO because of missing data. For instance, no data had been published on EO blood levels in ET-exposed mice, rats, or humans, with the exception of a study in rats [60] the reported data and methodology of which, however, were questioned [30]. Also missing were mouse-exposure studies with ET and only a few data had been reported with EO in mice.

In the model of Csanády et al. [20] both EO elimination pathways, the EH- and the GST-catalyzed one, were combined in a single pathway because it was the main emphasis of the work to estimate the tissue burdens of EO and the resulting hemoglobin-

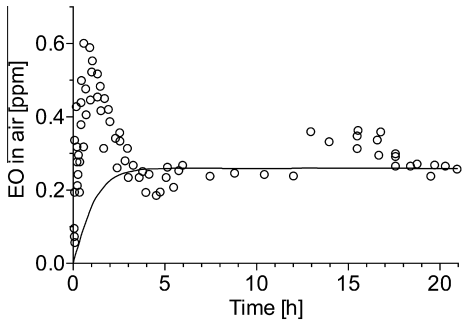

Fig. 1. Concentration–time course of metabolically produced ethylene oxide (EO) in the atmosphere of closed all-glass exposure chambers (6.4 L) each of which contained two male Sprague–Dawley rats (average body weight: 215 g) that were exposed for up to 21 h to ethylene at atmospheric concentrations of ET of >1000 ppm. Symbols: data measured in three independent experiments [32]; solid line, simulated by the PT model of Csanády et al. [20] under the assumption of the bioavailability of EO to be 45%.

and DNA-adduct levels, respectively, caused by exposures (up to 6 h/d) to ET at concentrations of up to 3000 ppm or EO at concentrations of up to 100 ppm (mice) or 300 ppm (rats). Depletion of GSH that was found in mice and rats at high EO concentrations (both species: [62]; mice: [12]) could not be predicted. Two PT models developed only for EO in male rats [55] or in mice, rats, and humans [29] described this effect. In both models, EH and GST catalyzed EO hydrolysis and EO conjugation with GSH, respectively, were modeled separately. Krishnan et al. [55] obtained the required enzyme parameters by model fits to in vivo data, whereas Fennell and Brown [29] used activities of EH and GST to EO that were derived from data in microsomes and cytosol of various tissues from mice and rats [11] and of livers from humans [29].

3.2. Existing biochemical parameters for model development

Enzyme- and substrate-specific biochemical parameters (such as V_{max} and K_m) determined in subcellular tissue fractions of laboratory animals and humans can be used in a PT model if their validity to adequately predict the kinetics of chemicals in vivo can be ensured [49]. In order to establish an experimental basis for the development of an upgraded PT model for ET and its metabolite EO, kinetics of the metabolism of ET and EO were investigated in tissue subcellular fractions of mice, rats, and humans.

3.2.1. ET-related parameters

CYP-mediated metabolism of ET was studied in microsomal incubations of male B6C3F1 mice, male F344 rats, and humans and determined as the production of EO [58]. Maximum EO formation rate (V_{maxCYP}) was highest in microsomes of mice and lowest in microsomes of humans. The highest apparent Michaelis constant of the CYP-catalyzed ET oxidation (K_{mCYP}) was found for rats. It was about 3fold higher than the values for mice and humans (Table 1).

ET destroys the hepatic CYP that catalyzes its oxidative metabolism by N-alkylation of one of the four pyrrole rings of the prosthetic heme [69,70]. Li et al. [58] calculated the elimination rate constant (k_{inhib}) of the suicide inhibition from fitting modeled concentration–time curves to monitored concentration–time courses of metabolically formed EO in incubations of ET in microsomal suspensions. The obtained values of k_{inhib} (Table 1) were rather high. They corresponded to half-lives of between 7.1 and 11.6 min.

The ET-oxidizing CYP isoenzyme is primarily CYP2E1 as was demonstrated in mice by comparing the EO formation in ET-exposed liver microsomes of CYP2E1-knockout animals with that of their wild-type counterpart [58]. In F344 rats, the importance of CYP2E1 for the metabolism of ET to EO was shown indirectly by Fennell et al. [30]. There are hints that CYP2E1 is also most relevant for the metabolism of ET in humans because the species-specific ratios of the values of V_{maxCYP}/K_{mCYP} to the values of V_{max}/K_m of the CYP2E1 activities (determined with chlorzoxazone as substrate; [22]) are very similar in liver microsomes of mice, rats, and humans.

Table 1
Parameters (mean values) of enzyme-catalyzed and non-enzymatic reactions in liver subcellular fractions of mice, rats, and humans with ethylene (ET) or ethylene oxide (EO) as substrates.

Parameter	Mouse	Rat	Human
Formation of EO from ET (microsomal incubations with ET)			
V_{maxCYP} (nmol EO/min/mg protein)	0.567	0.401	0.219
K_{mCYP} (mmol ET/L suspension)	0.0093	0.031	0.013
V_{maxCYP}/K_{mCYP} (µl/min/mg protein)	60.9	13.1	17.2
k_{inhib} (min^{-1})	0.060	0.070	0.098
Hydrolysis of EO (microsomal incubations with EO)			
V_{maxEH} (nmol EO/min/mg protein)	n.q.; 1.2*	n.q.; 1.8*	14.35
K_{mEH} (mmol EO/L suspension)	n.q.; 0.20*	n.q.; 0.20*	12.74
V_{maxEH}/K_{mEH} (µl/min/mg protein)	n.q.; 6.0*	n.q.; 9.0*	1.13
k_{hydrol} (min^{-1})	9.3×10^{-4}	9.3×10^{-4}	9.3×10^{-4}
EO conjugation with GSH (cytosolic incubations with EO)			
V_{maxGST} (nmol EO/min/mg protein)	251; 258*	47.7; 52.7*	10.3 (0.00–25.8)
K_{mGST} (mmol EO/L suspension)	9; 10.4*	9; 13.0*	9
V_{maxGST}/K_{mGST} (µl/min/mg protein)	27.9; 24.8*	5.3; 4.05*	1.14 (0.00–2.87)
k_{GSH} (min^{-1})	3.12×10^{-3}	3.12×10^{-3}	3.12×10^{-3}

All values are from Li et al. [58] except those marked by an asterisk (*), which are from Brown et al. [11].
Abbreviations: GSH, glutathione; n.q., not quantified because non-distinguishable from spontaneous hydrolysis; V_{maxCYP}, maximum rate of CYP2E1-catalyzed EO formation from ET; K_{mCYP}, apparent Michaelis constant of the reaction given as ET concentration; k_{inhib}, first-order rate constant of the ET-mediated suicide inhibition of CYP2E1; V_{maxEH}, maximum rate of epoxide hydrolase-catalyzed EO hydrolysis; K_{mEH}, apparent Michaelis constant of the reaction given as EO concentration; k_{hydrol}, first-order rate constant of the non-enzymatic hydrolysis of EO; V_{maxGST}, maximum rate of GSH S-transferase-catalyzed conjugation of EO with GSH; K_{mGST}, apparent Michaelis constant of the conjugation reaction given as EO concentration; k_{GSH}, pseudo first-order rate constant of the spontaneous conjugation of EO with GSH at a GSH concentration of 15 mmol/L in the incubation medium.

3.2.2. EO-related parameters

Kinetics of EO metabolism was investigated in tissue subcellular fractions prepared from B6C3F1 mice, F344 rats [11,58], and humans [58]. Metabolism of EO, catalyzed by EH, could be quantified and expressed as maximum rate of hydrolysis (V_{maxEH}) and corresponding Michaelis constant (K_{mEH}) only in microsomes of humans [58] (Table 1). Using liver microsomes of 5 human donors (both genders), Fennell and Brown [29] determined a mean EH activity with EO as substrate of 1.8 nmol/min/mg protein at an EO concentration of 15.4 mmol/L; however neither V_{max} nor K_m values were reported. For this EO concentration, a 4.4 higher EH activity of 7.9 nmol/min/mg protein can be calculated using the Michaelis–Menten equation and the values of V_{maxEH} and K_{mEH} obtained by Li et al. [58] with pooled microsomes of 25 donors (Table 1). The cause for the difference is unclear. In liver microsomes of mice and rats, Li et al. [58] could not distinguish the EH-mediated hydrolysis from the spontaneous, non-enzymatic hydrolysis that is characterized by the rate constant k_{hydrol} (Table 1). Also Brown et al. [11] found very low EH activities toward EO in liver microsomes of rats and mice (Table 1). The authors determined V_{maxEH} at an initial EO concentration of 15 mmol/L. The values of V_{maxEH} were not larger than the rate of

the non-enzymatic EO-hydrolysis at the same concentration of EO. The value of K_{mEH} in rats and mice could only be estimated.

EO was eliminated by GST-catalyzed and spontaneous conjugation with GSH in liver cytosol of the three species (Table 1). Non-enzymic conjugation of EO with GSH was also described by Brown et al. [11], but not quantified. In mouse or rat liver cytosol, both working groups [11] and [58] determined similar values of V_{maxGST} and K_{mGST}. There is also agreement between the values of V_{maxGST} and K_{mGST} determined by Li et al. [58] in cytosolic preparations of human livers and the mean GST activity toward EO of 8.9 nmol/min/mg protein at an EO concentration of 30 mmol/L, measured by Fennell and Brown [29] in liver cytosol of human donors. By means of the values of V_{maxGST} and K_{mGST} and using the Michaelis–Menten equation, an EO conjugation rate of 7.9 nmol/min/mg protein can be calculated for the EO concentration of 30 mmol/L. Li et al. [58] did not detect any GST activity with EO as substrate in cytosol of 2 out of the 13 human donors (Table 1). The finding was in agreement with the observation that 10–25% of non-Asians had GSTT1 null genotype [7].

Cytosolic GST activities toward EO were also quantified in kidneys of mice and rats of both sexes and in testes of both species [11]. There were no statistically significant gender differences in the activities of GST. Mean values of V_{maxGST} in kidneys of male mice and rats were 46.4 and 30.1s nmol/min/mg protein, respectively. Mean values of corresponding K_{mGST} were 7.1 (mouse) and 10.8 (rat) mmol/L. In testes, the values of V_{maxGST} were 17.3 (mouse) and 20.3 (rat) nmol/min/mg protein, those K_{mGST} were 8.1 (mouse) and 9.2 (rat) mmol/L.

3.2.3. Species differences in enzymatic activities

The species differences in the enzymatic activities (V_{max}/K_m) concerning the three reactions (Table 1) are consistent with frequent findings made in subcellular liver fractions that microsomal epoxidation of small olefins proceeds in humans at lower rates than in mice, microsomal EH-catalyzed hydrolysis of small epoxides is faster in humans than in both rodent species, and GSH conjugation of small epoxides by cytosolic GST occurs at the highest rates in mice. For epoxidation, see, e.g., Csanády et al. [18], 1,3-buatiene; Mendrala et al. [64], styrene; Seaton et al. [77], 1,2-epoxy-3-butene; Golding et al. [39], isoprene, 3,4-epoxy-3-methyl-1-butene, 3,4-epoxy-2-methyl-1-butene; Himmelstein et al. [44], 2-chloro-1,3-butadiene. For hydrolysis, see, e.g., Kreuzer et al. [54] or Csanády et al. [18], 1,2-epoxy-3-butene; Mendrala et al. [64], styrene-7,8-oxide; Boogaard and Bond [9], 1,2:3,4-diepoxybutane; Faller et al. [27], propylene oxide; Himmelstein et al. [44], (1-chloroethenyl)oxirane. For GSH conjugation, see, e.g., Kreuzer et al. [54], 1,2-epoxy-3-butene; Faller et al. [27], propylene oxide. Species differences in the activity of cytosolic GSTT1 in liver and kidney were investigated by Thier et al. [86]. The authors used methyl chloride and dichloromethane as substrates. Of the species investigated—mouse, rat, hamster, human (conjugators and non-conjugators)—GSTT1 activities were highest in mice (both organs).

3.3. Existing data for model validation

Filser et al. [35] quantified EO in venous blood of ET-exposed mice, rats, and humans at ET concentrations in air ranging from 1 to 10,000 ppm (animals) or from 5 to 50 ppm (humans). Fig. 2A and B depict concentration–time courses of EO measured in blood of animals exposed to ET concentrations of 30 ppm and higher. Also given are the time courses of EO exemplarily shown in the blood of one of the 4 ET-exposed volunteers (Fig. 2C). Up to concentrations of ET of about 100 ppm (animals) and 50 ppm (humans), EO concentrations in blood increased to plateaus that were reached 2–3 h after starting the exposures. At equal ET concentrations, blood levels of EO at plateau were in humans (Fig. 2D) at least 3 times and 6 times lower than in mice (Fig. 2A) and rats (Fig. 2B), respectively. At 300, 1000, and 10,000 ppm of ET, blood levels of EO in animals peaked shortly after starting the exposures. Thereafter, they declined to species-specific plateaus, the levels of which were similar regardless of whether the exposure concentration of ET was 300, 1000, or 10,000 ppm. In humans, the plateau levels differed interindividually by a factor of up to 1.51 (Fig. 2D). It was interpreted to result probably from the polymorphism of GSTT1 because a similar difference (factor 1.61) was found between carriers of the GSTT1 positive and GSTT1 null genotype in the EO-characteristic hemoglobin adduct levels of 32 cigarette smokers [28].

ET induced blood levels of EO in rats were also reported by two other groups. Fennell et al. [30] monitored EO concentrations in blood of male F344 rats at various time points during 6-h exposures to 300, 600, and 1000 ppm of ET. At 300 ppm, EO reached a maximum of about 0.08 μg/ml (1.8 μmol/L) followed by a decrease to about 0.06 μg/ml (1.4 μmol/L). At 600 ppm, EO increased to a peak concentration of roughly 0.13 μg/ml (3.0 μmol/L) after 1 h; then it decreased rapidly at first, then more slowly to a final EO concentration of 0.06 μg/ml (1.4 μmol/L). After 1 h of exposure to 1000 ppm of ET, EO reached a maximum concentration of about 0.11 μg/ml (2.5 μmol/L) followed by a slow decrease to 0.1 μg/ml (2.3 μmol/L) after 6 h. The data of Fennell et al. [30] are similar to those given in Fig. 2B with the exception that no peak was seen at 1000 ppm whereas such peaks were found by Filser et al. [35] at 300, 1000, and 10,000 ppm ET (Fig. 2B). Also in the studies of Filser and Bolt [32] an EO peak was found in the atmosphere of closed chambers that contained Sprague–Dawley rats exposed to ET concentrations of >1000 ppm (Fig. 1). Furthermore, EO peaked in blood of mice exposed to ET concentrations of between 300 and 10,000 ppm (Fig. 2A). The missing EO peak at 1000 ppm ET reported by Fennell et al. [30] is probably an incorrect result.

Maples and Dahl [60] determined EO in blood of male F344 rats that were exposed for 1 h to ET concentrations of 5 or 600 ppm. At 5 ppm, EO concentrations increased continuously to a plateau concentration of between 0.05 and 0.1 μg/g blood (1.1–2.3 μmol/L) reached after 14 min. At 600 ppm, EO rose quickly to a peak concentration of 3 μg/g blood (68 μmol/L), reached after about 7 min of exposure. About 4 to 5 min later, the EO concentration had dropped to a rather constant value of about 0.5 μg/g (11 μmol/L). The plateaus and the peak occurred much earlier and the reported EO concentrations were one order of magnitude higher than those found later by Fennell et al. [30] and Filser et al. [35]. The cause for the difference is not known. Fennell et al. [30] assumed problems of the analytical method used by Maples and Dahl [60] for the detection of EO.

Maples and Dahl [60] also exposed rats for up to 6 h to an ET concentration of 600 ppm. A small but significant decrease in the total hepatic CYP content was detected after 20 min (first measurement) and a larger one to 68% of the control value after 6 h (second measurement). The authors explained these results by the suicide inhibition of the ET-metabolizing CYP. Fennell et al. [30] extended the study by investigating total CYP content and CYP2E1 activity in F344 rats at ET exposure concentrations of 300, 600, and 1000 ppm, and additionally, the activities of the major CYP isoenzymes in hepatic microsomes of rats exposed to 1000 ppm of ET. Of the various CYP activities investigated, that of CYP2E1 showed the only consistent decrease in a concentration- and time-dependent manner. The CYP inactivation resulted from ET itself and not from its metabolite EO that did not reduce the hepatic CYP content of rats exposed to 5 ppm of EO [60]. This finding was in agreement with the observations that epoxides did not inactivate the CYP isoenzymes that became destroyed while metabolizing the corresponding olefins (reviewed by [16]).

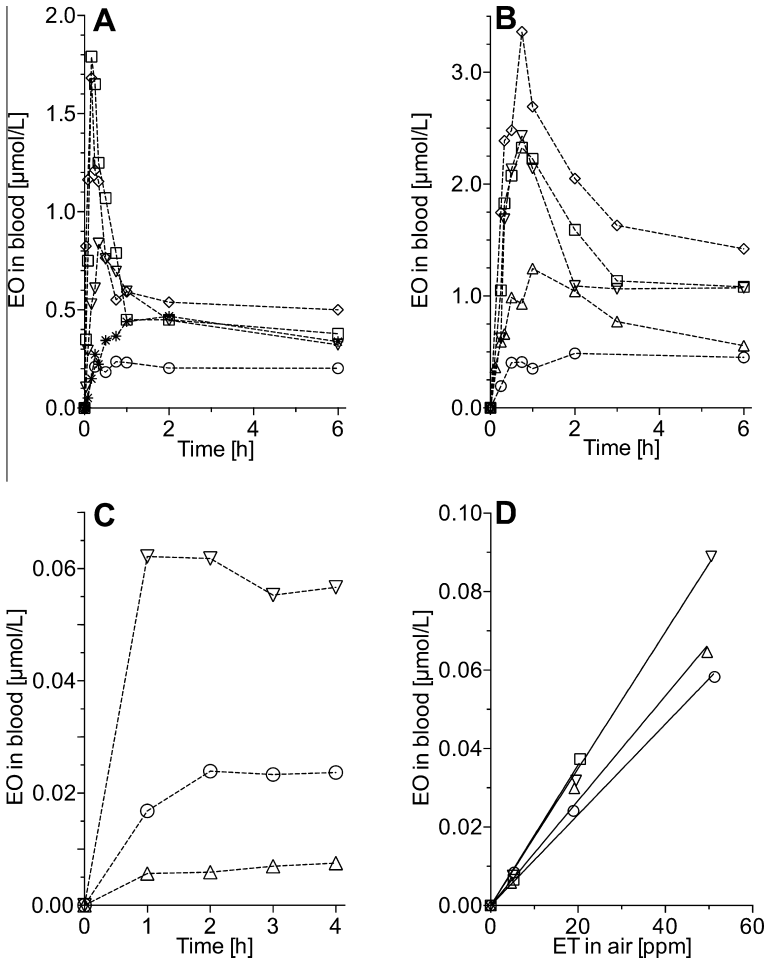

Fig. 2. Ethylene oxide (EO) in the venous blood of male B6C3F1 mice, male F344 rats, or male nonsmoking Caucasians exposed to constant concentrations of ethylene (ET); data from Filser et al. [35]. (A) and (B) Concentration–time courses of EO in the blood of mice (A) or rats (B) that were exposed up to 6 h to ET at atmospheric concentrations ranging from 30 up to 10,000 ppm. Symbols, mean values of EO concentrations measured in the blood of groups of up to three mice or rats immediately at the end of exposures to ET at concentrations of 30 (○), 100 (✳), 130 (△), 300 (▽), 1000 (□), and 10,000 (◇) ppm. (C) Concentration–time courses of EO in the blood of a human (volunteer A in Filser et al. [35] exposed to ET 3 times for 4 h. Symbols: mean values of measured EO concentrations monitored during exposures to ET at target concentrations of 5 (△), 20 (○), or 50 (▽) ppm. (D) Plateau concentrations of EO in the blood of 4 volunteers exposed to ET at target concentrations of 0 ppm (control values), 5 ppm, 20 ppm (volunteers A, B, C, and D), or 50 ppm (volunteers A, B, and C). Symbols: means of the measured plateau concentrations; A (○), B (▽), C (△), D (□). Solid lines: linear regressions through the origin.

Filser et al. [35] explained the results shown in Fig. 2 in the light of the studies of Maples and Dahl [60], Fennell et al. [30], and Li et al. [58] by an interaction between the CYP2E1-mediated formation of EO from ET, the suicide inhibition of CYP2E1 by ET, and the physiological turnover of CYP2E1. Immediately after starting an exposure to a high concentration of ET, the level of the metabolizing CYP2E1 decreases quickly due to the initial rapid inactivation by suicide inhibition. Later, a constant and clearly lower level is reached when the inactivation rate equals the CYP2E1 turnover rate. Concurrently, the initial rapid increase in EO blood levels decreases after reaching a maximum because EO metabolism becomes faster than its shrinking production. The elimination process, the rate of which depends on the actual EO concentration, slows with time until the plateau is reached at which both rates, EO production and EO elimination, are equal. At low ET concentrations, the turnover rate of CYP2E1 is high as compared to the rate of its destruction by suicide inhibition. As a consequence, EO in blood increases continuously until a plateau is attained. The in vivo data shown in Fig. 2 will be of utmost importance for testing the predictive capacity of a revised PT model for ET in rats, mice, and humans in whom the GSTT1 positive and negative individuals can also be reflected by the model.

3.4. Novel data for model validation

Concentration–time courses monitored in gas uptake studies are required for estimating metabolic parameters in the intact animal by fitting a classical compartmental or a PT model to the data and for testing the quality of a PT model with respect to the used metabolic parameters of a gaseous substance [76]. Gas uptake studies with ET [6] and with EO in male Sprague–Dawley rats [32] were used in the PT model of Csanády et al. [20]. The EO uptake data in male F344 rats [55] were used in three PT models [55,20,29]. Bearing in mind that B6C3F1 mice were used in the inhalation carcinogenicity study with EO and F344 rats in such studies with ET and EO, it would be meaningful to use data obtained in theses strains to validate a PT model for ET and EO. Therefore, gas uptake studies were carried out in the present work with ET and EO in B6C3F1 mice and with ET in F344 rats.

3.4.1. Gas uptake studies with ET

3.4.1.1. B6C3F1 mice. ET was administered at various initial concentrations in the atmosphere of closed chambers (2.8 L), each containing 5 naïve B6C3F1 mice. Fig. 3A shows the resulting concentration–time courses of ET (empty black circles) monitored

in the chamber air. Dashed lines connect the data points. At ET concentrations below 100 ppm, ET metabolism follows first-order kinetics with almost parallel slopes that are steeper than at higher concentrations. At a first glance, this picture seems to agree with simple saturation kinetics of the ET metabolism. A control experiment without animals revealed that the chambers were gas-tight and that humidified soda lime did not influence the ET concentration in the chamber air (▽ and blue line, fitted to the data by assuming an e-function). The loss of ET over time (calculated half-life 278 h) resulted most probably from the amount of ET sampled for GC analysis. The red symbols (△) together with the fitted e-function (red line) symbolize an ET-exposure experiment with 5 mouse carcasses. The calculated half-life (166 h) reflects a loss in the atmospheric ET concentration of only 1 ppm within almost 7 h. From a comparison of the concentration–time courses of ET seen in the control experiments with those obtained in the studies with living animals it follows clearly that the dose-dependent slopes of the continuous decreases of ET in the in vivo exposures resulted from intake and metabolism of ET.

In order to analyze the initial intake of ET up to its maximum enrichment in the body, a gas-uptake experiment was conducted with 5 mice pretreated with dithiocarbamate for inhibiting CYP2E1-mediated metabolism of ET (Fig. 3B). The curve, which was fitted to the measured data, shows a rapid decline followed by a plateau. The initial decline results from inhalation uptake of ET by the animals; the plateau is reached when the thermodynamic equilibrium (K_{eq}) between the ET concentrations in the bodies of the animals and in the air is attained. No further decrease of ET was seen in contrast to the picture with non-pretreated animals. It can be regarded as a proof for the effective inhibition of the ET-metabolism by dithiocarbamate. From the kinetic parameters describing the curve (see legend to the figure) and the volumes of the air space in the chamber (V_1, 637.5 ml) and of the exposed animals (V_2, 137.5 ml), the value of K_{eq} of ET for the mouse can be calculated by the following equation: $K_{eq} = [(y_{(0)} - y_{(\infty)}) \times V_1]/(V_2 \times y_{(\infty)}) \approx 0.5$. The value of the rate constant k (4.888 h^{-1}, see legend to the figure), which summarizes the intake process in the experiment, depends on the volumes V_1 and V_2, the breathing time volumes of the exposed animals, and the rate of transport of the lipophilic ET by the blood flow to its storage (the adipose tissue).

3.4.1.2. F344 rats. Fig. 4A depicts the results of the ET gas uptake studies performed in F344 rats (2 animals per exposure in a closed chamber of 6.4 L). Dashed lines connect the measured data (○). The picture resembles that seen in mice. The slopes of the concentration–time courses decrease with increasing initial ET concentrations. Also plotted in the figure is a control experiment with 2 rat carcasses (average body weight: 245 g) that were exposed in a closed chamber of 6.4 L to ET at an initial concentration of 30 ppm (△; red line, fitted e-function). The calculated half-life of 209 h resulted from a decrease in the ET concentration of less than 1 ppm within 6 h. For living rats, exposed at similar conditions to an initial ET concentration of 34 ppm (Fig. 4A), a half-life of ET in chamber air of 13.15 h was calculated. The 16-fold shorter half-life resulted clearly from metabolism of ET.

Also in rats, a gas-uptake experiment was conducted after inhibiting CYP2E1-mediated ET metabolism by pretreatment with dithiocarbamate. This procedure revealed the same drastic reduction of the biotransformation of ET (Fig. 4B) as was observed in mice. K_{eq} of ET in the rat was calculated from V_1 (4870 ml), V_2 (1500 ml), $y_{(0)}$ (430.8 ppm), and $y_{(\infty)}$ (383 ppm)—both concentrations gained from the e-function fitted to the measured data—to $K_{eq} \approx 0.4$. The value of the rate constant k was 4.337 h^{-1} (see legend to the figure).

3.4.1.3. Comparison with previous studies. Concentration–time courses of ET similar to those depicted in Figs. 3B and 4B had been obtained also in male Sprague–Dawley rats pretreated with dithiocarbamate. From the data, a value of K_{eq} of 0.7 was derived [6]. Using a PT model, Csanády et al. [20] estimated a value of 0.65. The K_{eq} values of 0.5 (mouse) and 0.4 (rat) calculated from the present data do not disagree with the older results.

The concentration–time courses of ET seen in naïve mice and rats (Figs. 3A and 4A) hint to saturation kinetics of ET in both species. From plotting such data (not shown in the original paper) to

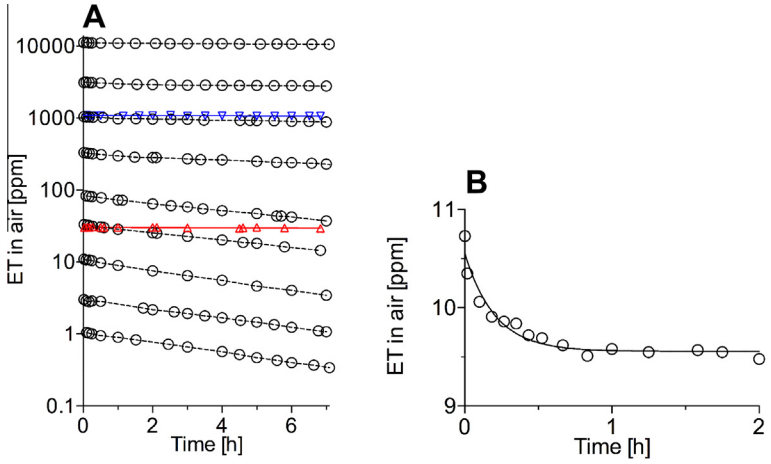

Fig. 3. Gas uptake studies with male B6C3F1 mice exposed to ethylene (ET) in closed all-glass chambers. (A) ET uptake by groups of 5 mice (average body weight: 27.5 g) placed in chambers (2.8 L) with initial concentrations of ET of 1.1, 3.0, 11, 33, 83, 330, 1050, 3110, or 11,200 ppm (○). Also shown are concentration–time courses of ET in a control experiment with humidified soda lime solely (▽) and in a control experiment with 5 mouse carcasses (average body weight: 26.1 g) exposed to ET at an initial concentration of 30.4 ppm (△). Symbols indicate measured concentrations of ET; dashed lines represent connections between data points; straight lines were fitted to the data by assuming e-functions the rate constants of which were 0.00249 h^{-1} (blue line) and 0.00417 h^{-1} (red line). (B) Concentration–time course of ET in the atmosphere of a chamber (0.8 L) containing a group of 5 mice (average body weight: 27.5 g) pretreated with the CYP2E1-inhibitor dithiocarbamate 30 min before start of exposure to ET. Symbols (○) indicate measured concentrations of ET. The solid black line shows the function $y = (y_{(0)} - y_{(\infty)}) \times e^{-kt} + y_{(\infty)}$ (with $y_{(0)} = 10.57$ ppm, $y_{(\infty)} = 9.56$ ppm, $k = 4.888$ h^{-1}), fitted to the data by using the program Prism 6 for Mac OS X from Graphpad Software, Inc., San Diego, California. The curve reflects the intake of ET until reaching the thermodynamic equilibrium between the ET concentrations in the organism and in the air.

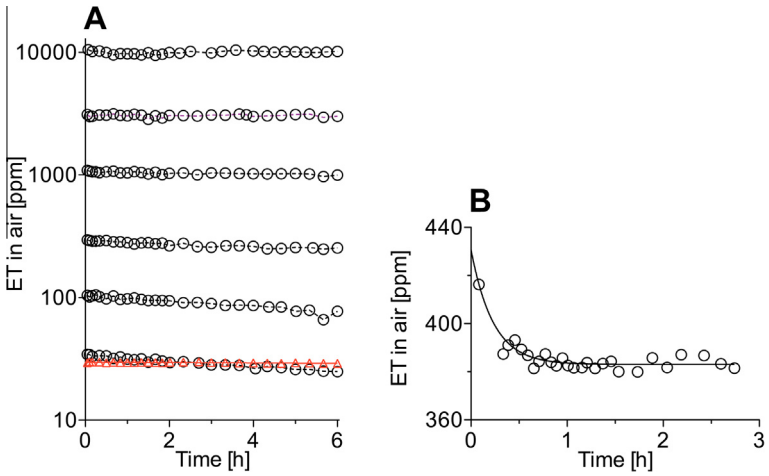

Fig. 4. Gas uptake studies with male F344 rats exposed to ethylene (ET) in closed all-glass chambers. (A) ET uptake by groups of 2 rats (average body weight: 300 g) placed in chambers (6.4 L) with initial target concentrations of ET of 34, 105, 295, 1090, 3110, or 10,500 ppm in air (○). Also shown are concentration–time courses of ET in a control experiment with 2 rat carcasses (average body weight: 245 g) exposed to ET at an initial concentration of 30 ppm (△). Symbols indicate measured concentrations of ET and dashed lines represent connections between data points. The red straight line was fitted to the data by assuming an e-function the rate constant of which was 0.00332 h^{-1}. (B) Concentration–time course of ET in the atmosphere of a chamber (6.4 L) containing a group of 5 rats (average body weight: 300 g) pretreated with the CYP2E1-inhibitor dithiocarbamate 30 min before start of exposure to ET (○). Symbols indicate measured concentrations of ET. The line shows the function $y = (y_{(0)} - y_{(\infty)}) \times e^{-kt} + y_{(\infty)}$ (with $y_{(0)}$ = 430.8 ppm, $y_{(\infty)}$ = 383 ppm, k = 4.337 h^{-1}), fitted to the data by using the program Prism 6 for Mac OS X from Graphpad Software, Inc., San Diego, California. The curve reflects the intake of ET until reaching the thermodynamic equilibrium between the ET concentrations in the organism and in the air.

the Eadie-Hofstee plot, Andersen et al. [3] derived a maximum rate of ET metabolism in male F344 rats of 0.24 mg/h/kg body weight, which is equivalent to 8.5 μmol/h/kg body weight (measured data not shown in the original publication). Bolt et al. [6] obtained the same value when analyzing in Sprague–Dawley rats similar ET-uptake data as the present ones by means of a compartment model. This value was also used in the PT model of Csanády et al. [20]. Based on the determination of EO in ET-exposed liver microsomal suspensions, Li et al. [58] calculated maximum in vivo rates of ET elimination—before suicide inhibition becomes effective—of 42.9 (mouse), 28.9 (rat), and 9.8 (human) μmol/h/kg body weight. The value for rats is 3.4 times higher than the one obtained by Andersen et al. [3] and Bolt et al. [6]. In the earlier determinations, the suicide inhibition, which pretends a lower maximum rate of ET metabolism, was not taken into account. One cause for the misinterpretation of the gas uptake curves at high ET concentrations was that the initial phase of CYP2E1 inhibition (see [58]) and the phase of ET enrichment in the organism (see Figs. 3B and 4B) are overlapping. Therefore, it was not possible to recognize the loss of the rate of ET metabolism. Obviously, precautions have to be taken when interpreting non-linear concentration–time courses obtained in gas uptake studies in which normally only the parent compound (here ET) is determined and not the direct metabolite (here EO) simultaneously. A reliable kinetic analysis of the ET data shown in Figs. 3A and 4A requires a PT model in which the species-specific CYP2E1 turnover and the rate constant of the ET-dependent suicide inhibition have to be incorporated. For that reason, an analysis on the sole basis of the measured concentration–time courses was not carried out.

3.4.2. Gas uptake studies with EO

EO uptake studies were required only for B6C3F1 mice; for F344 rats, such data had already been published [55]. Fig. 5 shows EO uptake studies in naïve mice and two control experiments, one without animals and one with EO-exposed mouse carcasses. The control experiment without animals but with humidified soda lime (25 g) in the chamber (6.4 L) showed a decrease of the EO concentration in air that followed first-order kinetics with a half-life of EO of 18.9 h. The EO loss from the chamber atmosphere resulted from the base-catalyzed hydrolysis of EO. This conclusion is supported by results of Filser and Bolt [32] who showed that the half-life of EO depended on the amount of soda lime. Also, the EO concentration remained constant over the exposure time in the absence of soda lime (data not shown). For the ET-exposure experiment with the carcasses of 5 mice a half-life of 7.6 h was calculated. The loss of atmospheric EO reflects most probably the slow intake of EO into the carcasses via the skin. It accumulates in the aqueous and in the lipid phase of the body. For the aqueous phase, a partition coefficient of EO in Tis-HCl buffer (pH 7.5; 37 °C) to EO in air of 62 was reported [83]. The adipose tissue/air partition coefficient

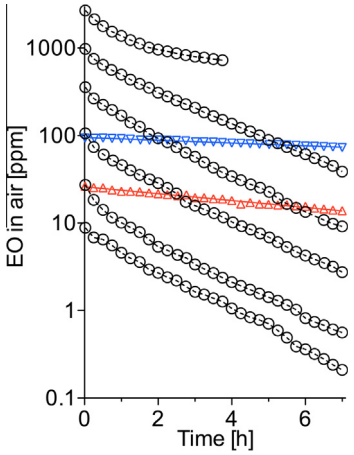

Fig. 5. Uptake of ethylene oxide (EO) by groups of 5 male B6C3F1 mice (average body weight: 27.5 g) placed in soda lime (25 g) containing closed all-glass chambers (6.4 L) with initial target concentrations of EO of 8.8, 27, 106, 360, 980, or 2700 ppm in air (○). A control experiment without animals but with humidified soda lime (25 g) in the chamber is represented by blue symbols (▽) and the blue straight line. Also shown is a concentration–time course of EO in a control experiment with 5 mouse carcasses (average body weight: 25.8 g) exposed to EO at an initial concentration of 26.5 ppm (red symbols (△) and red straight line). Symbols indicate measured concentrations of EO; dashed lines represent connections between data points. The straight lines were fitted to the data by assuming e-functions the rate constants of which were 0.03663 h^{-1} (blue line) and 0.0908 h^{-1} (red line).

of EO was determined to 43 at 37 °C [20]. For the human organism, Csanády et al. [20] calculated a K_{eq}-value of 53.

In the EO uptake studies with naïve mice, almost linearly decreasing parallel concentration–time courses were obtained in the semilogarithmic plot from the smallest initial EO concentration of 8.8 ppm up to an initial concentration of 360 ppm. This figure indicates that there was no saturation kinetics of the metabolic EO elimination within this concentration range. Somewhat flatter was the concentration decline following an initial EO concentration of 980 ppm. At the highest initial concentration of 2700 ppm EO, the concentration–time course flattened rapidly with the exposure time. The exposure was stopped after 3.75 h because the animals showed reduced physical activity. The linear concentration–time courses agree with in vitro findings [11,58] which showed that the GST-catalyzed EO conjugation with GSH was quantitatively by far the most relevant pathway of EO elimination in livers of mice and rats. In liver cytosol of both species, this process followed first-order kinetics of up to about 10 mmol EO per liter suspension. The non-linearity observed in vivo at the highest initial concentrations of EO hints at the depletion of the GSH pool in the liver as a result of its rapid consumption. A toxicokinetic analysis of the data presented in Fig. 5 requires a PT model with implemented GSH turnover as, for instance, was used in the models for butadiene [52], styrene [19,21], or EO [29]. In these models, the conjugation of an epoxide with GSH was described by a ping-pong mechanism. Csanády et al. [19] discussed explicitly the advantages of this mechanism over the second-order mechanism used in other PT models.

4. Conclusion

The data presented here will serve as an excellent basis for revising, extending, and validating the previously developed PT model for ET and EO in mouse, rat, and human [20]. This was recently exemplified for the rat when demonstrating a revised PT model for both substances at an international conference held in Austin, TX [50]. The PT model shall be published together with corresponding models for mice and humans (Filser et al.; in preparation).

Conflict of Interest

The authors have no conflict of interest.

Transparency Document

The Transparency document associated with this article can be found in the online version.

Acknowledgement

This work was supported in part by the Olefins Panel of the American Chemistry Council.

References

[1] ACC, American Chemistry Council's Olefin Panel, Olefins. <http://www.americanchemistry.com/ProductsTechnology/Olefins>, 2014 (accessed 10.10.2014).
[2] Alberta Environment, Assessment report on ethylene for developing ambient air quality objectives. ISBN No. 0-7785-2498-1 (online edition). <http://environment.gov.ab.ca/info/library/6721.pdf>, 2003 (accessed 05.09.2013).
[3] M.E. Andersen, M.L. Gargas, R.A. Jones, L.J. Jenkins Jr., Determination of the kinetic constants for metabolism of inhaled toxicants in vivo using gas uptake measurements, Toxicol. Appl. Pharmacol. 54 (1980) 100–116.
[4] J. Angerer, M. Bader, A. Kramer, Ambient and biochemical effect monitoring of workers exposed to ethylene oxide, Int. Arch. Occup. Environ. Health 71 (1998) 14–18.
[5] A.D. Arms, C.C. Travis, Reference Physiological Parameters in Pharmacokinetic Modeling, US-Environmental Protection Agency, Washington, DC, 1988 (Report Nr. EPA/600/6-88/004).
[6] H.M. Bolt, J.G. Filser, F. Störmer, Inhalation pharmacokinetics based on gas uptake studies. V. Comparative pharmacokinetics of ethylene and 1,3-butadiene in rats, Arch. Toxicol. 55 (1984) 213–218.
[7] H.M. Bolt, R. Thier, Relevance of the deletion polymorphisms of the glutathione S-transferases GSTT1 and GSTM1 in pharmacology and toxicology, Curr. Drug Metab. 7 (2006) 613–628.
[8] H.M. Bolt, J.G. Filser, Olefinic hydrocarbons: a first risk estimate for ethene, Toxicol. Pathol. 12 (1984) 101–105.
[9] P.J. Boogaard, J.A. Bond, The role of hydrolysis in the detoxification of 1,2:3,4-diepoxybutane by human, rat, and mouse liver and lung in vitro, Toxicol. Appl. Pharmacol. 141 (1996) 617–627.
[10] P.J. Boogaard, P.S.J. Rocchi, N.J. van Sittert, Biomonitoring of exposure to ethylene oxide and propylene oxide by determination of haemoglobin adducts: correlations between airborne exposure and adduct levels, Int. Arch. Occup. Environ. Health 72 (1999) 142–150.
[11] C.D. Brown, B.A. Wong, T.R. Fennell, In vivo and in vitro kinetics of ethylene oxide metabolism in rats and mice, Toxicol. Appl. Pharmacol. 136 (1996) 8–19.
[12] C.D. Brown, B. Asgharian, M.J. Turner, T.R. Fennel, Ethylene oxide dosimetry in the mouse, Toxicol. Appl. Pharmacol. 148 (1998) 215–221.
[13] F. Brugnone, L. Perbellini, G. Faccini, F. Pasini, Concentration of ethylene oxide in the alveolar air of occupationally exposed workers, Am. J. Ind. Med. 8 (1985) 67–72.
[14] F. Brugnone, L. Perbellini, G.B. Faccini, F. Pasini, G.B. Bartolucci, E. DeRosa, Ethylene oxide exposure. Biological monitoring by analysis of alveolar air and blood, Int. Arch. Occup. Environ. Health 58 (1986) 105–112.
[15] J.P. Conkle, B.J. Camp, B.E. Welch, Trace composition of human respiratory gas, Arch. Environ. Health 30 (1975) 290–295.
[16] M.M. Correia, P.R. Ortiz de Montellano, Inhibition of cytochrome P450 enzymes, in: P.R. Ortiz de Montellano (Ed.), Cytochrome P450: Structure, Mechanism, and Biochemistry, Kluwer Academic/Plenum Publishers, New York, NY, 2005, pp. 247–322.
[17] COT, Committee on toxicity of chemicals in food, consumer products and the environment, COT statement on physiologically based pharmacokinetic modelling. COT Statement 2003/05December 2003. <http://www.food.gov.uk/sites/default/files/cot/pbpkstatement.pdf>, 2003 (accessed 29.12.2014).
[18] G.A. Csanády, F.P. Guengerich, J.A. Bond, Comparison of the biotransformation of 1,3-butadiene and its metabolite, butadiene monoepoxide, by hepatic and pulmonary tissues from humans, rats and mice, Carcinogenesis 13 (1992) 1143–1153.
[19] G.A. Csanády, A.L. Mendrala, R.J. Nolan, J.G. Filser, A physiologic pharmacokinetic model for styrene and styrene-7,8-oxide in mouse, rat and man, Arch. Toxicol. 68 (1994) 143–157.
[20] G.A. Csanády, B. Denk, C. Pütz, P.E. Kreuzer, W. Kessler, C. Baur, M.L. Gargas, J.G. Filser, A physiological toxicokinetic model for exogenous and endogenous ethylene and ethylene oxide in rat, mouse, and human: formation of 2-hydroxyethyl adducts with hemoglobin and DNA, Toxicol. Appl. Pharmacol. 165 (2000) 1–26.
[21] G.A. Csanády, W. Kessler, H.D. Hoffmann, J.G. Filser, A toxicokinetic model for styrene and its metabolite styrene-7,8-oxide in mouse, rat and human with special emphasis on the lung, Toxicol. Lett. 138 (2003) 75–102.
[22] M.H. Court, L.L. von Moltke, R.I. Shader, D.J. Greenblatt, Biotransformation of chlorzoxazone by hepatic microsomes from humans and ten other mammalian species, Biopharm. Drug Dispos. 18 (1997) 213–226.
[23] B. Denk, Abschätzung des kanzerogenen Risikos von Ethylenoxid für den Menschen durch Speziesextrapolation von der Ratte unter Berücksichtigung der Pharmakokinetik, GSF-Bericht 20/90, München, Germany, 1990.
[24] U. Duus, S. Osterman-Golkar, M. Törnqvist, J. Mowrer, S. Holm, L. Ehrenberg, Studies of determinants of tissue dose and cancer risk from ethylene oxide exposure, in: Proceedings of the Symposium on Management of Risk from Genotoxic Substances in the Environment, Solna, Sweden, 1989, pp. 141–153.
[25] L. Ehrenberg, M. Törnqvist, The research background for risk assessment of ethylene oxide: aspects of dose, Mutat. Res. 330 (1995) 41–54.
[26] I. Eide, R. Hagemann, K. Zahlsen, E. Tareke, M. Törnqvist, R. Kumar, P. Vodicka, K. Hemminki, Uptake, distribution and formation of hemoglobin and DNA adducts after inhalation of C2–C8 1-alkenes (olefins) in the rat, Carcinogenesis 16 (1995) 1603–1609.
[27] T.H. Faller, G.A. Csanády, P.E. Kreuzer, C.M. Baur, J.G. Filser, Kinetics of propylene oxide metabolism in microsomes and cytosol of different organs from mouse, rat, and humans, Toxicol. Appl. Pharmacol. 172 (2001) 62–74.
[28] T.R. Fennell, J.P. MacNeela, R.W. Morris, M. Watson, C.L. Thompson, D.A. Bell, Hemoglobin adducts from acrylonitrile and ethylene oxide in cigarette smokers: effects of glutathione S-transferase T1-null and M1-null genotypes, Cancer Epidemiol. Biomarkers Prev. 9 (2000) 705–712.
[29] T.R. Fennell, C.D. Brown, A physiologically based pharmacokinetic model for ethylene oxide in mouse, rat, and human, Toxicol. Appl. Pharmacol. 173 (2001) 161–175.
[30] T.R. Fennell, R.W. Snyder, C. Parkinson, J. Murphy, R.A. James, The effect of ethylene exposure on ethylene oxide in blood and on hepatic cytochrome P450 in Fischer rats, Toxicol. Sci. 81 (2004) 7–13.

[31] J.G. Filser, H.M. Bolt, Exhalation of ethylene oxide by rats on exposure to ethylene, Mutat. Res. 120 (1983) 57–60.
[32] J.G. Filser, H.M. Bolt, Inhalation pharmacokinetics based on gas uptake studies. VI. Comparative evaluation of ethylene oxide and butadiene monoxide as exhaled reactive metabolites of ethylene and 1,3-butadiene in rats, Arch. Toxicol. 55 (1984) 219–223.
[33] J.G. Filser, The closed chamber technique – uptake, endogenous production, excretion, steady-state kinetics and rates of metabolism of gases and vapors, Arch. Toxicol. 66 (1992) 1–10.
[34] J.G. Filser, B. Denk, M. Törnqvist, W. Kessler, L. Ehrenberg, Pharmacokinetics of ethylene in man; body burden with ethylene oxide and hydroxyethylation of hemoglobin due to endogenous and environmental ethylene, Arch. Toxicol. 66 (1992) 157–163.
[35] J.G. Filser, W. Kessler, A. Artati, E. Erbach, T. Faller, P.E. Kreuzer, Q. Li, J. Lichtmannegger, W. Numtip, D. Klein, C. Pütz, B. Semder, G.A. Csanády, Ethylene oxide in blood of ethylene-exposed B6C3F1 mice, Fischer 344 rats, and humans, Toxicol. Sci. 136 (2013) 344–358.
[36] V. Fiserova-Bergerova, Modeling of metabolism and excretion in vivo, in: V. Fiserova-Bergerova (Ed.), Modeling of Inhalation Exposure to Vapors: Uptake, Distribution, and Elimination, vol. 1, CRC Press Inc., Boca Raton, FL, 1983, pp. 101–132.
[37] R.H. Garman, W.M. Snellings, R.R. Maronpot, Brain tumors in F344 rats associated with chronic inhalation exposure to ethylene oxide, Neurotoxicology 6 (1985) 117–138.
[38] R.H. Garman, W.M. Snellings, R.R. Maronpot, Frequency, size and location of brain tumours in F-344 rats chronically exposed to ethylene oxide, Food Chem. Toxicol. 24 (1986) 145–153.
[39] B.T. Golding, L. Cottrell, D. Mackay, D. Zhang, W.P. Watson, Stereochemical and kinetic comparisons of mono- and diepoxide formation in the in vitro metabolism of isoprene by liver microsomes from rats, mice, and humans, Chem. Res. Toxicol. 16 (2003) 933–944.
[40] J.H. Graham, R.G. Linderman, Ethylene production by ectomycorrhizal fungi, *Fusarium oxysporum* f. sp. *pini*, and by aseptically synthesized ectomycorrhizae and *Fusarium*-infected Douglas-fir roots, Can. J. Microbiol. 26 (1980) 1340–1347.
[41] F. Granath, O. Rohlén, C. Göransson, L. Hansson, A.L. Magnusson, M. Törnqvist, Relationship between dose in vivo of ethylene oxide and exposure to ethene studied in exposed workers, Hum. Exp. Toxicol. 15 (1996) 826–833.
[42] F.P. Guengerich, D.-H. Kim, M. Iwasaki, Role of human cytochrome P-450 IIE1 in the oxidation of many low molecular weight cancer suspects, Chem. Res. Toxicol. 4 (1991) 168–179.
[43] T.E. Hamm Jr., D. Guest, J.G. Dent, Chronic toxicity and oncogenicity bioassay of inhaled ethylene in Fischer-344 rats, Fundam. Appl. Toxicol. 4 (1984) 473–478.
[44] M.W. Himmelstein, S.C. Carpenter, P.M. Hinderliter, Kinetic modeling of β-chloroprene metabolism: I. In vitro rates in liver and lung tissue fractions from mice, rats, hamsters, and humans, Toxicol. Sci. 79 (2004) 18–27.
[45] IARC, International Agency for Research on Cancer, Ethylene. Some industrial chemicals, IARC Monographs on the Evaluation of Carcinogenic Risks to Humans, vol. 60, WHO, IARC Press, Lyon, France, 1994, pp. 45–71.
[46] IARC, International Agency for Research on Cancer, Ethylene oxide. Some industrial chemicals, IARC Monographs on the Evaluation of Carcinogenic Risks to Humans, vol. 60, WHO, IARC Press, Lyon, France, 1994, pp. 73–159.
[47] IARC, International Agency for Research on Cancer, Ethylene oxide. 1,3-Butadiene, ethylene oxide and vinyl halides (vinyl fluoride, vinyl chloride and vinyl bromide, IARC Monographs on the Evaluation of Carcinogenic Risks to Humans, vol. 97, WHO, IARC Press, Lyon, France, 2008, pp. 185–309.
[48] IARC, International Agency for Research on Cancer, Ethylene oxide. Chemical agents and related occupations. A review of human carcinogens, IARC Monographs on the Evaluation of Carcinogenic Risks to Humans, vol. 100F, WHO, IARC Press, Lyon, France, 2012, pp. 379–400.
[49] IPCS, International Programme on Chemical Safety, Characterization and application of physiologically based pharmacokinetic models in risk assessment, (IPCS harmonization project document; No. 9), WHO, 2010.
[50] IISRP, International Institute of Synthetic Rubber Producers, Inc., International Symposium – Understanding the health risks of lower olefins, November 5–6 2014, IISRP, Houston, TX, 2014.
[51] J. Jankovic, W. Jones, J. Burkhart, G. Noonan, Environmental study of firefighters, *Ann. Occup. Hyg.* 35 (1991) 581–602.
[52] G. Johanson, J.G. Filser, A physiologically based pharmacokinetic model for butadiene and its metabolite butadiene monoxide in rat and mouse and its significance for risk extrapolation, Arch. Toxicol. 67 (1993) 151–163.
[53] A. Kautiainen, M. Törnqvist, Monitoring exposure to simple epoxides and alkenes through gas chromatographic determination of hemoglobin adducts, Int. Arch. Occup. Environ. Health 63 (1991) 27–31.
[54] P.E. Kreuzer, W. Kessler, H.F. Welter, C. Baur, J.G. Filser, Enzyme specific kinetics of 1,2-epoxybutene-3 in microsomes and cytosol from livers of mouse, rat and man, Arch. Toxicol. 65 (1991) 59–67.
[55] K. Krishnan, M.L. Gargas, T.R. Fennell, M.E. Andersen, A physiologically based description of ethylene oxide dosimetry in the rat, Toxicol. Ind. Health 8 (1992) 121–140.
[56] G.D. Lawrence, G. Cohen, In vivo production of ethylene from 2-keto-4-methylthiobutyrate in mice, Biochem. Pharmacol. 34 (1985) 3231–3236.
[57] J. Lewalter, N-alkylvaline levels in globin as a new type of biomarker in risk assessment of alkylating agents, Int. Arch. Occup. Environ. Health 68 (1996) 519–530.
[58] Q. Li, G.A. Csanády, W. Kessler, D. Klein, H. Pankratz, C. Pütz, N. Richter, J.G. Filser, Kinetics of ethylene and ethylene oxide in subcellular fractions of lungs and livers of male B6C3F1 mice and male Fischer 344 rats and of human livers, Toxicol. Sci. 123 (2011) 384–398.
[59] D.W. Lynch, T.R. Lewis, W.J. Moorman, J.R. Burg, D.H. Groth, A. Khan, L.J. Ackerman, B.Y. Cockrell, Carcinogenic and toxicologic effects of inhaled ethylene oxide and propylene oxide in F344 rats, Toxicol. Appl. Pharmacol. 76 (1984) 69–84.
[60] K.R. Maples, A.R. Dahl, Levels of epoxides in blood during inhalation of alkenes and alkene oxides, Inhal. Toxicol. 5 (1993) 43–54.
[61] J.L. Martin, D.J. Caldwell, Evaluation of a sampling method for the measurement of occupational exposure to ethylene, J. Occup. Environ. Hyg. 1 (2004) 363–370.
[62] J.A. McKelvey, M.A. Zemaitis, The effect of ethylene oxide (EO) exposure on tissue glutathione levels in rats and mice, Drug Chem. Toxicol. 9 (1986) 51–66.
[63] R.L. Melnick, Carcinogenicity and mechanistic insights on the behavior of epoxides and epoxide-forming chemicals, Ann. N.Y. Acad. Sci. 982 (2002) 177–189.
[64] A.L. Mendrala, P.W. Langvardt, K.D. Nitschke, J.F. Quast, R.J. Nolan, In vitro kinetics of styrene and styrene oxide metabolism in rat, mouse, and human, Arch. Toxicol. 67 (1993) 18–27.
[65] National Research Council, Guide for the Care and Use of Laboratory Animals, National Academy Press, Washington, DC, 2011.
[66] M.J.M. Nivard, K. Czene, D. Segerbäck, E.W. Vogel, Mutagenic activity of ethylene oxide and propylene oxide under *XPG* proficient and deficient conditions in relation to *N*-7-(2-hydroxyalkyl)guanine levels in Drosophila, Mutat. Res. 529 (2003) 95–107.
[67] NOVA Chemicals, Product risk profile ethylene. <http://www.novachem.com/ExWeb%20Documents/responsible-care/ETHYLENERP.pdf>, 2012 (accessed 05.09.2013).
[68] NTP, US National Toxicology Program, Toxicology and carcinogenesis studies of ethylene oxide (CAS No. 75-21-8) in B6C3F1 mice (inhalation studies). NTP Technical Report No. 326; NIH Publication No. 88-2582, Research Triangle Park, NC, 1987.
[69] P.R. Ortiz de Montellano, B.A. Mico, Destruction of cytochrome P-450 by ethylene and other olefins, Mol. Pharmacol. 18 (1980) 128–135.
[70] P.R. Ortiz de Montellano, H.S. Beilan, K.L. Kunze, B.A. Mico, Destruction of cytochrome P-450 by ethylene. Structure of the resulting prosthetic heme adduct, J. Biol. Chem. 256 (1981) 4395–4399.
[71] S. Osterman-Golkar, L. Ehrenberg, Covalent binding of reactive intermediates to hemoglobin as an approach for determining the metabolic activation of chemicals—ethylene, Drug Metab. Rev. 13 (1982) 647–660.
[72] S. Osterman-Golkar, B. Farmer, D. Segerbäck, E. Bailey, C.J. Calleman, K. Svenson, L. Ehrenberg, Dosimetry of ethylene oxide in the rat by quantitation of alkylated histidine in hemoglobin, Teratog. Carcinog. Mutagen. 3 (1983) 395–405.
[73] D. Potter, D. Blair, R. Davies, W.P. Watson, A.S. Wright, The relationship between alkylation of haemoglobin and DNA in Fischer 344 rats exposed to [^{14}C]ethylene oxide, Arch. Toxicol. Suppl. 13 (1989) 254–257.
[74] S.B. Primrose, Ethylene-forming bacteria from soil and water, J. Gen. Microbiol. 97 (1976) 343–346.
[75] G. Ram Chandra, M. Spencer, A micro apparatus for absorption of ethylene and its use in determination of ethylene in exhaled gases from human subjects, Biochim. Biophys. Acta 69 (1963) 423–425.
[76] M.B. Reddy, R.S.H. Yang, H.J. Clewell III, M.E. Andersen (Eds.), Physiologically based pharmacokinetic (PBPK) modeling – Science and applications. Chapter 2 "Halogenated Alkanes", section 2.3 "Experimental methods demonstrated for groups of chemicals", John Wiley and Sons, Inc., Hoboken, NJ, 2005. pp. 26–29.
[77] M.J. Seaton, M.H. Follansbee, J.A. Bond, Oxidation of 1,2-epoxy-3-butene to 1,2:3,4-diepoxybutane by cDNA-expressed human cytochromes P450 2E1 and 3A4 and human, mouse and rat liver microsomes, Carcinogenesis 16 (1995) 2287–2293.
[78] G.A. Sega, P.A. Brimer, E.E. Generoso, Ethylene oxide inhalation at different exposure-rates affects binding levels in mouse germ cells and hemoglobin. Possible explanation for the effect, Mutat. Res. 249 (1991) 339–349.
[79] D. Segerbäck, Alkylation of DNA and hemoglobin in the mouse following exposure to ethene and ethene oxide, Chem. Biol. Interact. 45 (1983) 139–151.
[80] D. Segerbäck, Reaction products in hemoglobin and DNA after *in vitro* treatment with ethylene oxide and *N*-(2-hydroxyethyl)-*N*-nitrosourea, Carcinogenesis 11 (1990) 307–312.
[81] M.C.C. Serra, A.M. Mainar, A.M.F. Palavra, Solubility of ethene in water and in a medium for the cultivation of a bacterial strain, J. Chem. Eng. Data 56 (2011) 1596–1601.
[82] J. Shen, W. Kessler, B. Denk, J.G. Filser, Metabolism and endogenous production of ethylene in rat and man, Arch. Toxicol. Suppl. 13 (1989) 237–239.
[83] G. Schmiedel, J.G. Filser, H.M. Bolt, Rat liver microsomal transformation of ethene to oxirane in vitro, Toxicol. Lett. 19 (1983) 293–297.
[84] W.M. Snellings, C.S. Weil, R.R. Maronpot, A two-year inhalation study of the carcinogenic potential of ethylene oxide in Fischer 344 rats, Toxicol. Appl. Pharmacol. 75 (1984) 105–117.
[85] D.K. Spracklin, M.E. Emery, K.E. Thummel, E.D. Kharasch, Concordance between trifluoroacetic acid and hepatic protein trifluoroacetylation after disulfiram inhibition of halothane metabolism in rats, Acta Anaesthesiol. Scand. 47 (2003) 765–770.
[86] R. Thier, F.A. Wiebel, A. Hinkel, A. Burger, T. Brüning, K. Morgenroth, T. Senge, M. Wilhelm, T.G. Schulz, Species differences in the glutathione transferase GSTT1-1 activity towards the model substrates methyl chloride and dichloromethane in liver and kidney, Arch. Toxicol. 72 (1998) 622–629.

[87] R. Thier, H.M. Bolt, Carcinogenicity and genotoxicity of ethylene oxide: new aspects and recent advances, Crit. Rev. Toxicol. 30 (2000) 595–608.
[88] M.A. Törnqvist, J.G. Almberg, E.N. Bergmark, S. Nilsson, S.M. Osterman-Golkar, Ethylene oxide doses in ethene-exposed fruit store workers, Scand. J. Work Environ. Health 15 (1989) 436–438.
[89] F. Vandenbussche, D. Van Der Straeten, The role of ethylene in plant growth and development, Annu. Plant Rev. 44 (2012) 219–242.
[90] J.S. Vergnes, I.M. Pritts, Effects of ethylene on micronucleus formation in the bone marrow of rats and mice following four weeks of inhalation exposure, Mutat. Res. 324 (1994) 87–91.
[91] K. Victorin, M. Ståhlberg, A method for studying the mutagenicity of some gaseous compounds in *Salmonella typhimurium*, Environ. Mol. Mutagen. 11 (1988) 65–77.
[92] V.E. Walker, T.R. Fennel, P.B. Upton, T.R. Skopek, V. Prevost, D.E. Shuker, J.A. Swenberg, Molecular dosimetry of ethylene oxide: formation and persistence of 7-(2-hydroxyethyl)guanine in DNA following repeated exposures of rats and mice, Cancer Res. 52 (1992) 4328–4334.
[93] V.E. Walker, J.P. MacNeela, J.A. Swenberg, M.J. Turner Jr., T.R. Fennel, Molecular dosimetry of ethylene oxide: formation and persistence of *N*-(2-hydroxyethyl)valine in hemoglobin following repeated exposures of rats and mice, Cancer Res. 52 (1992) 4320–4327.
[94] V.E. Walker, K.Y. Wu, P.B. Upton, A. Ranasinghe, N. Scheller, M.H. Cho, J.S. Vergnes, T.R. Skopek, J.A. Swenberg, Biomarkers of exposure and effect as indicators of potential carcinogenic risk arising from in vivo metabolism of ethylene to ethylene oxide, Carcinogenesis 21 (2000) 1661–1669.
[95] K.Y. Wu, A. Ranasinghe, P.B. Upton, V.E. Walker, J.A. Swenberg, Molecular dosimetry of endogenous and ethylene oxide-induced *N*7-(2-hydroxyethyl) guanine formation in tissues of rodents, Carcinogenesis 20 (1999) 1787–1792.
[96] K.Y. Wu, N. Scheller, A. Ranasinghe, T.Y. Yen, R. Sangaiah, R. Giese, J.A. Swenberg, A gas chromatography/electron capture/negative chemical ionization high-resolution mass spectrometry method for analysis of endogenous and exogenous *N*7-(2-hydroxyethyl)guanine in rodents and its potential for human biological monitoring, Chem. Res. Toxicol. 12 (1999) 722–729.
[97] K.Y. Wu, S.Y. Chiang, W.C. Shih, C.C.J. Huang, M.F. Chen, J.A. Swenberg, The application of mass spectrometry in molecular dosimetry: ethylene oxide as an example, Mass Spectrom. Rev. (2011), http://dx.doi.org/10.1002/mas.20299.